

Investigation of the brittle failure properties of an A42 pipeline steel butt weld : comparison of the base metal, simulated HAZ and weld metal

L. Lam Thanh¹, R. Piques¹, A.F. Gourgues¹, R. Batisse², P. Wident³

¹ Centre des Matériaux, ENSMP, UMR CNRS 7633, BP 87, 91003 Evry cedex, France

² Gaz de France 361 av. du Président Wilson B.P. 33, 93211 La Plaine Saint Denis, France

³ CEA/Saclay CEREM/SRMA 91191 Gif/Yvette Cedex, France

ABSTRACT: Assessing a flaw acceptability in a welded structure by means of a failure assessment diagram (FAD) can be difficult when accurate data (K_{mat} , local behaviors) on the heterogeneous materials of the weld are not available. The aim of this work is to demonstrate that the coarse grained heat affected zone (CGHAZ) is the critical microstructure of the studied weld and to study the behavior mismatch of the different materials. Therefore bending tests on as received weld blanks were conducted and showed failure initiation in the CGHAZ. This microstructure was reproduced using a GLEEBLE 1500 thermal simulator. Charpy V-Notch tests on weld metal (W-M), base metal (B-M) and simulated CGHAZ were made showing the brittleness of the CGHAZ and the mismatch diminution with increasing σ_y . Smooth tensile tests on B-M and W-M showed the same mismatch evolution.

INTRODUCTION

The welding process creates in the base metal (B-M) a heat affected zone (HAZ) in the vicinity of the weld metal (W-M). As the temperature history varies continuously in the HAZ only small size domains of homogeneous microstructure are found. When assessing a flaw acceptability in such a welded structure, the complex microstructure features and the residual stresses may lead to the necessity of using high security factors because of the lack of accurate data. The paper attempts to investigate the brittle failure conditions of a pipeline steel butt weld. The failure properties can rely on both the microstructure properties and the mismatch between the W-M and the B-M. The

coarse grained heat affected zone (CGHAZ), in most cases [1] [2] but not all [3], [4] is the most critical material. Therefore this study focuses on showing that for the studied weld the CGHAZ is the most critical microstructure and on studying the B-M and W-M behavior mismatch in order to improve estimates of the local loading of the weld.

First, bending tests on as received weld blanks were performed at low temperature to determine in which microstructure the brittle failure initiates. As these tests showed failure initiation in the CGHAZ, this microstructure was reproduced by thermal treatment on volumes big enough to machine sub-sized Charpy V-notched specimens (CVN). The CVN energies of the B-M, W-M and CGHAZ were compared at various temperatures and the acquired load displacement curves showed the mismatch (M) evolution with the yield strength (σ_y). Tensile tests showed the same evolution. The work is still in progress on applying the local approach to predict the weld failure but the present study already shows how the CGHAZ is undeniably the critical microstructure.

PROCEDURE

Butt welded pipeline parts (6 pass welding) were provided by Gaz de France, their wall thickness is of 10mm and the pipeline diameter is 500mm. The materials are presented in the next section.

Four points bending tests on the weld itself were performed using an INSTRON servo hydraulic testing machine equipped with a temperature control system. Full thickness specimens (fig.1 a) were cut out of the pipe-line butt weld and the tests were performed at -196°C in order to obtain brittle failure. Due to the low thickness of the pipe sub-sized Charpy V-notched (CVN) specimens were used (fig.1b). The W-M specimens were cut from moulds filled with this material. The CGHAZ specimens were prepared by applying a thermal cycle to 60 * 11 * 8mm³ B-M blanks, using a GLEEBLE 1500 thermal simulator. All the specimens were cut in the same directions (T-L) of the pipe (fig.4). The tests were performed on an instrumented pendulum of 300J at the CEA/SRMA.

B-M and W-M tensile tests (fig.1c) were also performed between -196°C and +100°C under the quasi-static regime ($\dot{\epsilon} = 5.10^{-4}$).

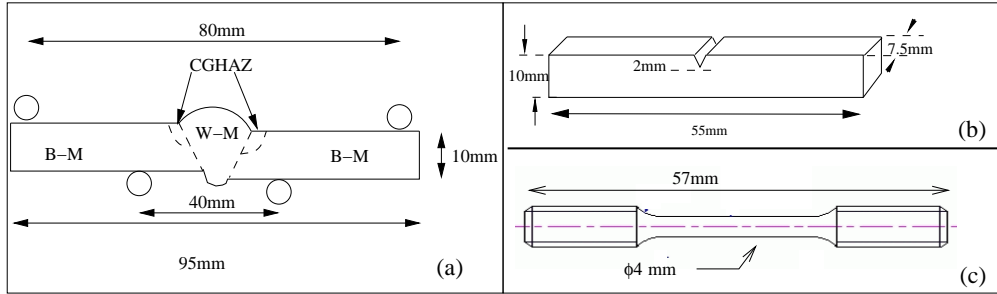


Figure 1: (a) Four point bending of the weld with misalignment and geometrical discontinuities; (b) CVN specimen; (c) Smooth tensile specimen

MATERIALS

The B-M were cut from the welded pipeline far away from the weld. The W-M was deposited in moulds (20mm thickness) in order to obtain large enough volumes of material to machine specimens. The base and weld metals compositions are given in table 1 whereas welding conditions are given in table 2.

TABLE 1: Chemical composition of the base and weld metals (weight %) and mean micro hardness over six measurements.

	C	S	Si	P	Cr	Ni	Mn	hardness $HV_{0.1}$
B-M	0.14	0.012	0.18	0.010	0.01	0.01	0.67	157
W-M	0.14	0.006	0.23	0.009	0.04	0.008	0.68	185

The base metal microstructure is composed of ferrite and pearlite (fig.2). A segregated band is found at mid thickness of the plate and elongated ($\approx 100\mu m$) MnS stringers are found all over the wall thickness. The weld metal is ferritic with small carbides at the grain boundaries. The CGHAZ is a mix of upper bainite, ferrite and pearlite. Its mean micro-hardness is 173 $HV_{0.1}$.

RESULTS and DISCUSSION

Four point bending tests were performed on as received weld blanks. The two welded parts were mis-aligned ($\approx 1mm$) and the last welding pass created a geometrical discontinuity at the surface of the CGHAZ. Nevertheless these tests showed that when testing the whole weld the failure initiates in the

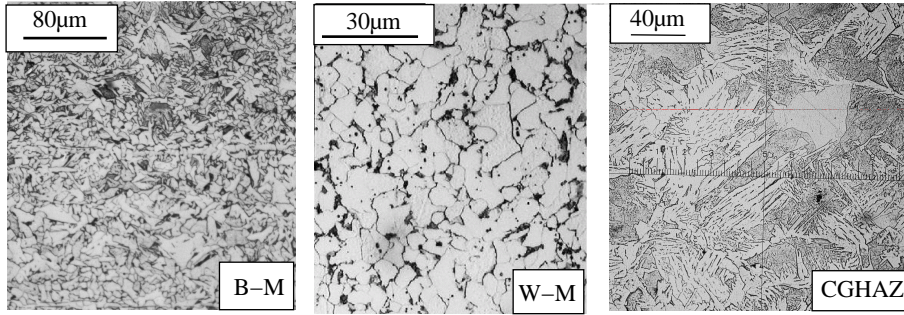


Figure 2: Microstructures of the base metal, the weld metal and the CGHAZ.

CGHAZ (fig.3). Secondary cracking was evidenced on the load/displacement curves by pop-in phenomena and on polished etched (nital 4%) cross-sections of fractured welds. These secondary cracks are all located in the CGHAZ, this is an other evidence of the brittleness of the CGHAZ.

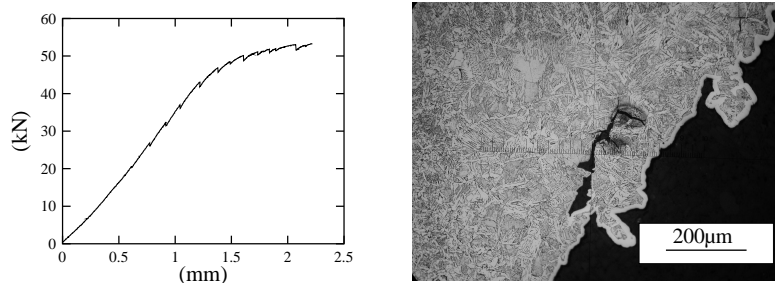


Figure 3: Four point bending load displacement curve and secondary cracking in the CGHAZ.

The CGHAZ microstructure was simulated using a Gleeble 1500 thermal simulator. First, Rosenthal analysis [5] (eq. 1) was used to estimate the temperature evolution in the CGHAZ and so to obtain the peak temperature (T_P) and the cooling criterion ($\Delta t_{T_1}^{T_2}$) needed to use Rykaline's thermal cycles (eq. 2). The parameters of equation 1 were fitted in order to reproduce the temperature evolution experimentally measured during the last pass welding sequence (fig.4).

$$T - T_0 = \frac{H \cdot V_a}{2 \cdot \pi \cdot \Gamma \cdot r_a} \cdot \exp \left(-V_a \frac{\zeta}{2 \cdot k} \right) \cdot \exp \left(-V_a \frac{r_a}{2 \cdot k} \right) \quad (1)$$

$$\theta = \frac{1}{\frac{1}{T_2-T_0} - \frac{1}{T_1-T_0}} \quad T_1 = 800^\circ C \quad T_2 = 500^\circ C$$

$$T(t, T_P, \Delta t_{T_2}^{T_1}) = T_0 + \theta \cdot \frac{\Delta t_{T_2}^{T_1}}{t} \cdot \exp \left(\frac{-\Delta t_{T_2}^{T_1}}{e.t} \cdot \frac{\theta}{T_P - T_0} \right) \quad (2)$$

TABLE 2: Welding conditions and parameters used to simulate the HAZ thermal cycles

Power	(UI) 3900 W
Output	(η) 0.6
Speed of the arc	(V_a) 2.6mm/s
Thermal conductivity	$\Gamma = 0.028 \text{ J/mm}^\circ\text{C}$
Specific volumic heat	$\rho_c = 0.0044 \text{ J/mm}^3 \cdot ^\circ\text{C}$
Plate thickness	$t=10\text{mm}$
Inter pass temperature	$T_0 = 150^\circ\text{C}$
Thermocouple distance	$y=5\text{mm}, z=8\text{mm}$
$H = \frac{U.I.\eta}{V_a}$	$k = \frac{\Gamma}{\rho_c}$
$\zeta = x - V_a t$	$r_a^2 = \zeta^2 + y^2 + z^2$

This equation was applied with the parameters fitted for a point located in the CGHAZ region. This first thermal cycle was applied to blanks cut from the base metal, and subsequently modified so that the simulated CG-HAZ microstructure (fig 4) matched the actual weld CGHAZ with respect of phases, hardness, and crystallography (EBSD). The CGHAZ does not exhibit a banded microstructure but the base metal does. To reduce this effect a first temperature peak at 1300°C followed by a rapid cooling ($\Delta t_{500}^{800} = 5\text{s}$) was necessary to obtain a more homogeneous microstructure. Afterwards, a second thermal cycle $T_P = 1200^\circ\text{C}$ $\Delta t_{500}^{800} = 19\text{s}$ enabled to obtain the desired microstructure.

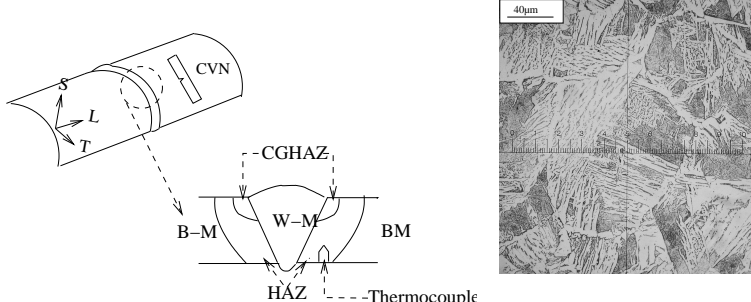


Figure 4: Thermocouple location during welding (left), Simulated CG-HAZ(right)

The Charpy ductile to brittle transition (DBT) curves are shown in figure 5. The CVN energy decreases in the ductile regime when temperature increases,

so the regular \tanh curves could not be fitted to the data sets. The function used to describe the impact energy versus temperature is given in eq.3 from [6] where L represents lower shelf value and H(T) the so called upper shelf value which is allowed to decrease with temperature.

$$CVN(T) = \frac{L+H(T)}{2} + \frac{H(T)-L}{2} * \tanh\left(\frac{T-T_0}{c}\right) \quad (3)$$

$$H(T) = H_0 - k(T - T_0)$$

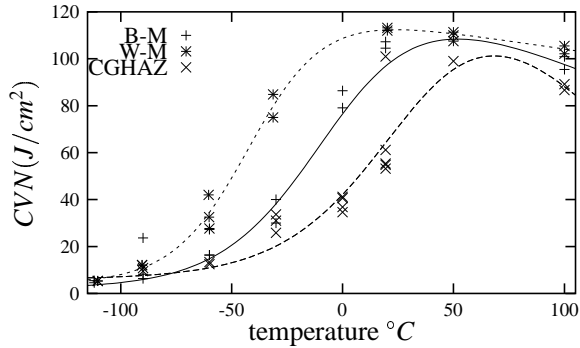


Figure 5: Charpy DBT transition curves

These DBT curves show that between -60°C and 50°C (DBT) the CGHAZ is the most brittle material. The CGHAZ is still brittle at 20°C , whereas the B-M and the W-M are already ductile. Even in the upper shelf the CGHAZ impact energy is the lowest. So in terms of material properties the failure is most likely to occur in the CGHAZ.

At lower temperatures (brittle regime, $T < 60^{\circ}\text{C}$) the impact energy is fairly the same for the B-M and CGHAZ, in fact the failure occurs for very small displacements, the energies are very low and it is not possible to conclude from these tests whether the CGHAZ is more brittle than the B-M or not.

The load displacement curves of these tests (fig.6) show that the W-M over-reaches the base metal at temperatures above -60°C . But this over-matching decreases with temperature and the B-M and W-M are even-matched at -60°C under dynamic loading. The same phenomenon was observed with smooth tensile tests on the B-M and W-M (fig 7) : The mismatch decreases with temperature and the two materials are even matched at -196°C . This temperature is lower than for the CVN tests because the phenomenon is enhanced by the dynamic loading.

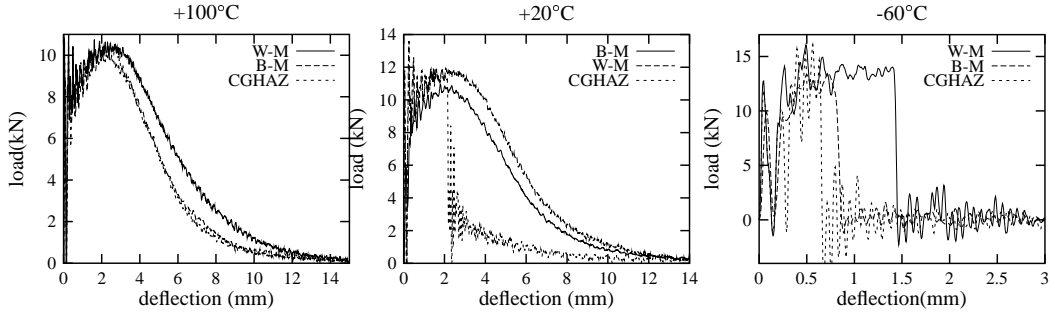


Figure 6: Load / deflection curves of the instrumented Charpy tests

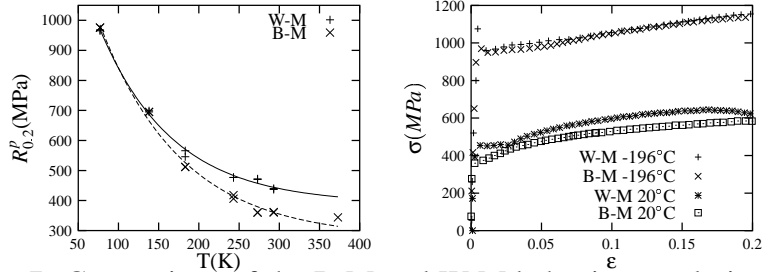


Figure 7: Comparison of the B-M and W-M behaviors evolution with temperature : $R_{0.2}^P$ proof stress (left) and stress strain curves (right)

As has reported in [2] the MnS stringers are not modified by the welding heat treatment. Therefore the B-M and simulated CGHAZ have similar failure modes but not at the same temperatures because of the brittle microstructure of CGHAZ. In the upper-shelf the failure occurs by lamellar tearing around the MnS stringers. In the DBT domain this lamellar tearing enables the stress concentration needed for the onset of cleavage (fig.8).

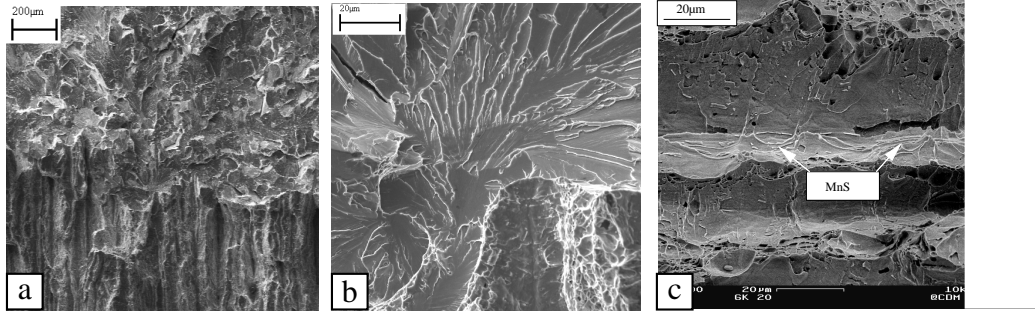


Figure 8: Failure mode of the CGHAZ in the DBT a) transition lamellar tearing to cleavage; b) cleavage initiation in front of a lamellar tearing crack; c) MnS inclusions inside lamellar tearing cracks

CONCLUSIONS

1. The CGHAZ is the most brittle material of the butt-welded joint.
2. The failure of weld is governed by the failure of the CGHAZ.
3. The weld mismatch is a function of temperature and strain rate. This has to be taken into account because the local strain and stress state in the CGHAZ is influenced by the mismatch.

Further work is actually in progress in order to apply the local approach to predict the failure of the weld. This work focuses on modeling the behavior and brittle failure criterion for the various weld constituents (B-M, W-M, CG-HAZ).

ACKNOWLEDGMENT: *The authors are very grateful to B. Marini of the CEA/SRMA.*

REFERENCES

1. Moltubakk, T., Thaulow, C. and Zhang, Z. (1999) *Engineering Fracture Mechanics*, **62**, 445–462.
2. Chae, D., Young, C., Goto, D. and Koss, D. (2001) *Metallurgical and Materials Transactions A*, **32A**, 2229–2237.
3. Kim, J., Oh, Y. and Hwang, I. (2001) *Journal of Nuclear Materials*, **299**, 132–139.
4. Gianetto, J. (1998). In: *5th conference on trends in welding research*. ASM International, ed J.M. Vitek.
5. Rosenthal, D. (1935). In: *II^e Congres National des Sciences de Bruxelles*, pp. 1278–1291.
6. Kohout, J. (2001). In: *Charpy centenary conference*, pp. 81–88, volume 1.